

Title	Quantitative evaluation of the degradation amount of the silane coupling layer of CAD/CAM resin composites by water absorption
Author(s)	Lee, Chunwoo; Yamaguchi, Satoshi; Imazato, Satoshi
Citation	Journal of Prosthodontic Research. 2023, 67(1), p. 55-61
Version Type	VoR
URL	<a href="https://hdl.handle.net/11094/93096">https://hdl.handle.net/11094/93096</a>
rights	© 2023 Japan Prosthodontic Society. All rights reserved.
Note	

*Osaka University Knowledge Archive : OUKA*

<https://ir.library.osaka-u.ac.jp/>

Osaka University

# Quantitative evaluation of the degradation amount of the silane coupling layer of CAD/CAM resin composites by water absorption

Chunwoo Lee, Satoshi Yamaguchi<sup>\*</sup>, Satoshi Imazato

Department of Biomaterials Science, Osaka University Graduate School of Dentistry, Osaka, Japan

## Abstract

**Purpose:** Degradation of silane coupling layers by water ingress in computer-aided design/computer-aided manufacturing (CAD/CAM) of resin composites has been reported qualitatively. In this study, we quantitatively evaluated how water absorption of CAD/CAM resin composites affects the silane coupling layer by *in vitro* and *in silico* methods.

**Methods:** A Katana Avencia block (KAB) and an experimental matrix block composed of only a matrix resin were used to evaluate the effect of water immersion for seven days on the elastic modulus. X-ray photoelectron spectroscopy (XPS) with fluorine-labeling of the KAB was performed to evaluate the atomic percentage of F1s, which represents the hydrolysis amount by water immersion. *In silico* analysis of the three-dimensional model of the KAB was performed to determine the coupling ratios before and after water immersion.

**Results:** The elastic modulus of the KAB was 8.2 GPa before and 6.9 GPa after immersion in water. The atomic percentages of F1s in the after- and before-immersion groups were 14.31% and 11.52%, respectively, suggesting that hydrolysis of the silane coupling layer occurred during water immersion. From *in silico* analysis of the three-dimensional model of the KAB, the coupling ratio was predicted to be 78.2% before water immersion. After water immersion, the coupling ratio was predicted to be 68.4%.

**Conclusions:** The *in vitro* and *in silico* approaches established in this study were able to predict the silane coupling ratios of CAD/CAM resin composites, and they showed that the silane coupling ratio decreased by water absorption.

**Keywords:** Computer-aided design/computer-aided manufacturing resin composite block, Finite element analysis, Silane coupling, Water absorption

Received 23 September 2021, Accepted 25 November 2021, Available online 29 December 2021

## 1. Introduction

Computer-aided design/computer-aided manufacturing (CAD/CAM) systems have been widely used in dentistry[1–3] since the first dental CAD/CAM restoration was reported in the 1980s[4,5]. CAD/CAM resin composites consist of a matrix resin and inorganic fillers treated with a silane coupling agent[6–8]. The matrix resin forms the basis of the composite structure and is composed of organized methacrylate-derived polymers, such as urethane dimethacrylate (UDMA), bisphenol A-glycidyl methacrylate, or triethylene glycol dimethacrylate (TEGDMA)[7]. Inorganic fillers, which are commonly made of silica, zirconia, and alumina, can be used to reinforce the composite structure because of their excellent mechanical properties[9–11]. For CAD/CAM resin composites, 0.1 μm or smaller nano-fillers composed of chemically stable inorganic materials are often used to improve the mechanical properties and provide polishability to create a smooth surface[12–16]. Because inorganic fillers are chemically stable, surface modification using silane coupling agents

is required to adhere the fillers to the organic matrix resin[17–19]. γ-Methacryloyloxypropyl trimethoxysilane (γ-MPTS) is a typical silane coupling agent, and it forms a 1.9–3.0-nm-thick layer between fillers and the matrix resin[20,21].

Water ingress leads to hydrolytic breakdown of the bonds between the silane and filler particles[22,23]. This water-induced degradation negatively affects the restoration longevity and mechanical properties[6,22–25]. While degradation of silane coupling layers has been qualitatively reported, the quantitative details have not been revealed because arbitrary control of the silane coupling ratio of the filler is not possible with conventional *in vitro* tests.

Rigorous mathematical theories of homogenization have been proposed for quantitative analysis of composite materials[26–28]. These theories assume that the material properties are periodic functions of the micro-scale variables, where the period is very small compared with the macro-scale variables. With this assumption, the equivalent macro-scale material properties can be calculated from known or arbitrary micro-scale properties. In dentistry, *in silico* homogenization analysis has been used to investigate multi-factorial issues, such as the effect of the nano-filler particle diameter on the physical properties of CAD/CAM resin composites[28].

*In vitro* high-resolution imaging enables analysis of nano-scale

DOI: [https://doi.org/10.2186/jpr.JPR\\_D\\_21\\_00236](https://doi.org/10.2186/jpr.JPR_D_21_00236)

\*Corresponding author: Satoshi Yamaguchi, Department of Biomaterials Science, Osaka University Graduate School of Dentistry, 1-8 Yamadaoka, Suita, Osaka 565-0871, Japan.

E-mail address: [yamaguchi.satoshi.dent@osaka-u.ac.jp](mailto:yamaguchi.satoshi.dent@osaka-u.ac.jp)

Copyright: © 2021 Japan Prosthodontic Society. All rights reserved.

**Table 1.** Compositions of the materials used

Materials (Manufacturer)	Code	Monomer	Filler	Filler Content (vol%)
Katana Avencia Block (Kuraray Noritake Dental)	KAB	UDMA <sup>‡</sup> , TEGDMA <sup>‡‡</sup>	SiO <sub>2</sub> (40 nm)* Al <sub>2</sub> O <sub>3</sub> (20 nm)	55
Experimental Matrix Block	EMB	UDMA <sup>‡</sup> , TEGDMA <sup>‡‡</sup>	-	-

<sup>‡</sup> UDMA: urethane dimethacrylate

<sup>‡‡</sup> TEGDMA: triethylene glycol dimethacrylate

\*average diameter

structures, and it produces an accurate model reflecting the morphological composition. *In silico* homogenization allows arbitrary control of the properties, which enables identification of the main factor of physico-mechanical issues at the macro-scale. Therefore, the combination of *in vitro* and *in silico* approaches may enable quantitative investigation of degradation of CAD/CAM resin composites by water absorption.

The aim of this study was to quantitatively evaluate how water absorption of CAD/CAM resin composites affects the silane coupling layer by *in vitro* and *in silico* methods.

## 2. Materials and Methods

### 2.1. Materials

A Katana Avencia block (KAB; Kuraray Noritake Dental, Tokyo, Japan) and an experimental matrix block (EMB; Kuraray Noritake Dental) were used (**Table 1**). The EMB was composed of only a matrix resin consisting of UDMA and TEGDMA, and used to calculate elastic modulus of the matrix resin. It was manufactured at the same temperature and pressure as the KAB, excluding fillers (**Fig. 1**).

### 2.2. Three-point bending test

The three-point bending test was performed to evaluate the elastic modulus of the KAB and EMB before and after immersion in water. The blocks were sliced into 14-mm × 4.0-mm × 1.2-mm slices with a low-speed precision cutter (IsoMet, Buehler, IL, USA). Ten specimens were left untreated as the before-immersion group, and another ten specimens were stored in distilled water for seven days at 37°C as the after-immersion group. The three-point bending test was performed with a universal testing machine (EZ-SX, Shimadzu, Kyoto, Japan). The maximum load was 500 N and the crosshead speed was 1 mm/min.

The *in silico* non-linear finite element analysis (NLFEA) method was performed to determine the elastic moduli of the materials. The three-point bending test environment was simulated with NLFEA software (LS-DYNA, Ansys, PA, USA). The simulation parameters were the flexural strain, density, and arbitrary elastic modulus. The flexural strain was taken from the result of the *in vitro* three-point bending test. The density was directly calculated by dividing the weight of the specimen measured with a precision digital weighing scale (GR-120, A&D, Tokyo, Japan) by the volume of the specimen estimated by micro-computed tomography (R<sub>m</sub>CT2, Rigaku, Tokyo, Japan). *In silico* three-point bending analysis was repeatedly performed by changing the elastic modulus. When the root mean squared error of the load in the *in vitro* and *in silico* load–displacement curve was less than 1 N, the arbitrary elastic modulus was determined as the true

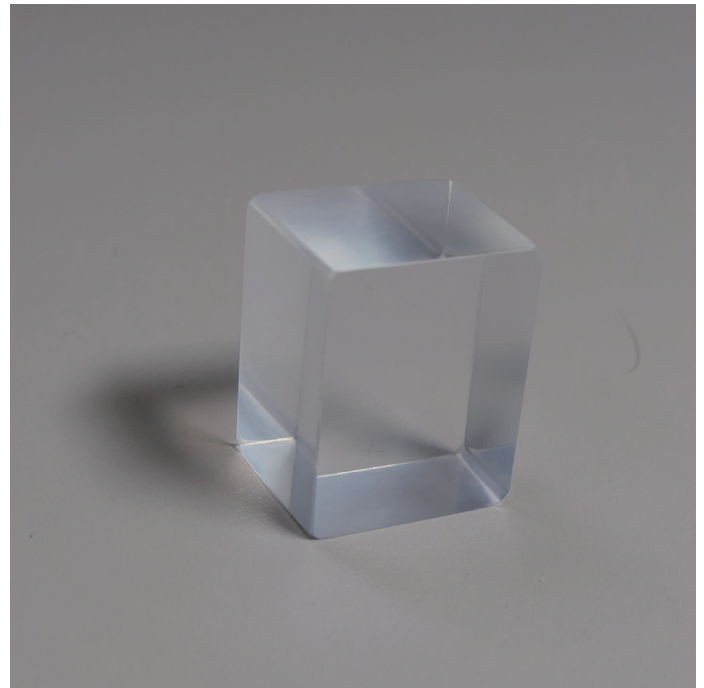


**Fig. 1.** Experimental block made only of the resin matrix. The size of the block was 18 mm × 15 mm × 15 mm.

elastic modulus of the material (**Fig. 2**).

### 2.3. XPS investigation

The KAB block was sliced into 7.0-mm × 4.0-mm × 1.2-mm slices with a low-speed precision cutter (IsoMet). Five specimens were allocated to the before-immersion group (control, no treatment) and after-immersion group, where the specimens were immersed in distilled water for seven days at 37°C. The specimens of both groups were subject to a decontamination process by boiling in 5 wt% sodium peroxodisulfate (Na<sub>2</sub>S<sub>2</sub>O<sub>8</sub>) solution for 15 min, followed by ultrasonic rinsing with 70% ethanol. 1H,1H,2H,2H-perfluorooctyldimethylchlorosilane (PFODMCS; C<sub>10</sub>H<sub>10</sub>ClF<sub>13</sub>Si, FUJIFILM Wako Chemicals, Osaka, Japan) was used for fluorine labeling (**Fig. 3**). The specimens were treated with 5% PFODMCS solution in 99% ethanol for 2 h at 60°C. The effectiveness of the fluorine-labeling process was determined by energy-dispersive X-ray spectroscopy (EDX). An XPS (JPS-9010, JEOL, Tokyo, Japan) investigation was performed to evaluate the amount of fluorine by the atomic percentage of F1s.

The atomic percentages of F1s in the before- and after-immersion specimens were analyzed by a Student's *t*-test with a level of statistical significance of  $\alpha = 0.05$  using statistical analysis software (IBM SPSS Statistics 24, IBM Corp., Armonk, NY, USA).

### 2.4. In silico analysis

A three-dimensional model of the KAB was taken from a previous study (**Fig. 4**)<sup>[30]</sup>. Five sub-models of a 100 nm cube were randomly extracted from the original three-dimensional model for the calculation because of computational power limitations, and the 2 nm silane space was applied around the fillers (**Fig. 5**). Eleven coupling ratios (100%, 95%, 90%, 85%, 80%, 75%, 70%, 65%, 60%, 55%,

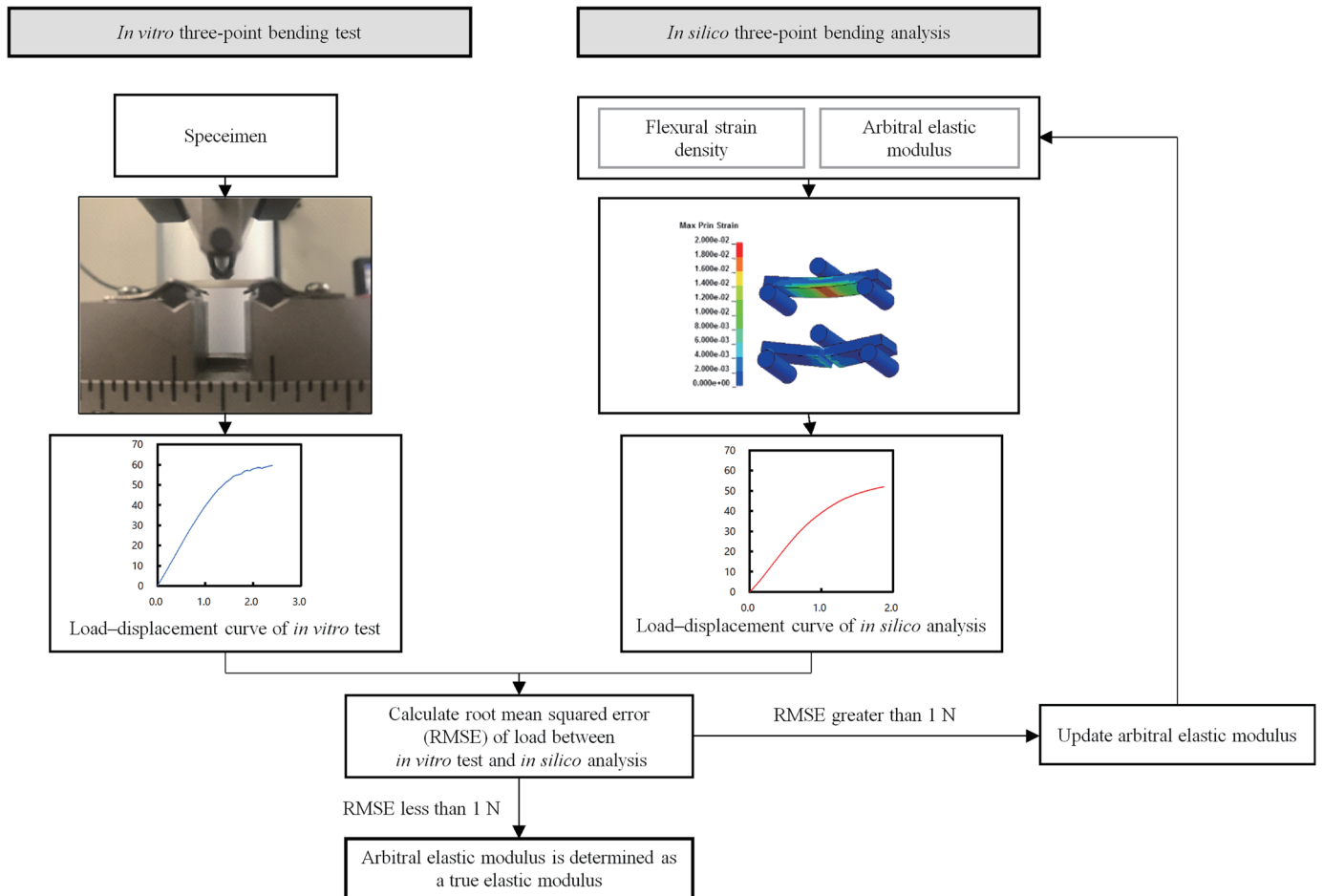


**Fig. 2.** Scheme for determining the true elastic modulus

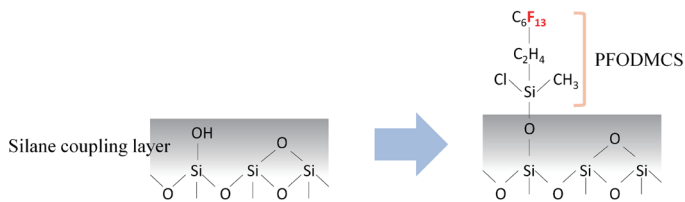


**Fig. 3.** Schematic illustration of molecular interaction between silane coupling layer and 1H-1H-2H-2H-perfluorooctylmethylchlorosilane

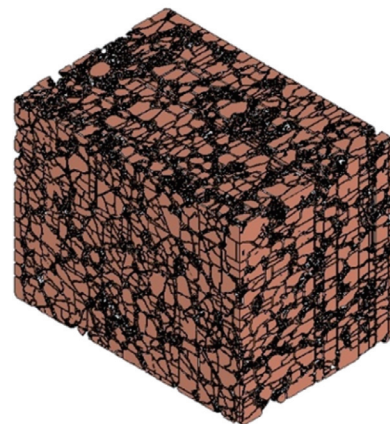


**Fig. 4.** Three-dimensional KAB model. The size of the model was  $1.8 \mu\text{m} \times 1.4 \mu\text{m} \times 1.2 \mu\text{m}$ . A three-dimensional model of the KAB was taken from a previous study[29].

and 50%) of the silane coupling layer and the corresponding elastic moduli were calculated with voxel-based finite element analysis (FEA) software (VOXELCON2015, Quint, Tokyo, Japan).

To determine the coupling ratio, *in silico* homogenization analysis was performed with sub-models of the 100-nm cube in three steps. First, the elastic modulus of the sub-model ( $EM_{\text{model}}$ ) was calculated with the elastic modulus of the matrix ( $EM_{\text{matrix}}$ ), elastic modulus of the filler ( $EM_{\text{filler}}$ ), and arbitrary elastic modulus of the silane coupling layer ( $arbEM_{\text{silane}}$ ) using the voxel-based FEA software. Second, if  $EM_{\text{model}}$  and the elastic modulus of the block ( $EM_{\text{block}}$ ) were the same,  $arbEM_{\text{silane}}$  was considered to be the true elastic modulus of the silane coupling layer ( $EM_{\text{silane}}$ ) and the third step was per-

formed. Otherwise,  $arbEM_{\text{silane}}$  was updated and the first step was repeated. In the third step, the coupling ratio was determined with  $EM_{\text{silane}}$  using the elastic modulus and coupling ratio of the silane coupling layer relation described above.

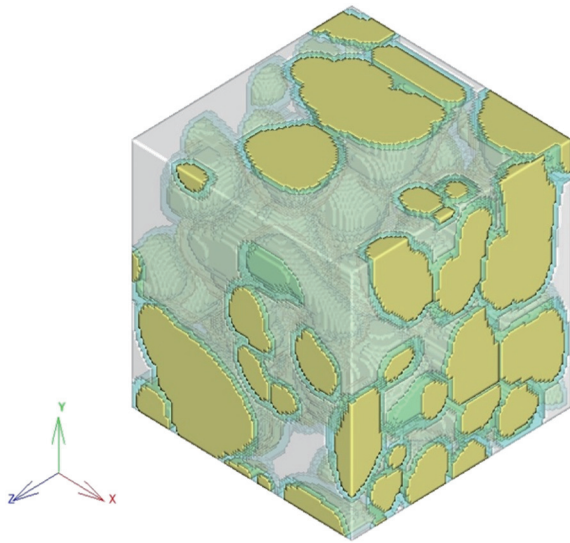


**Fig. 5.** Cubic sub-model of the KAB (100 nm)

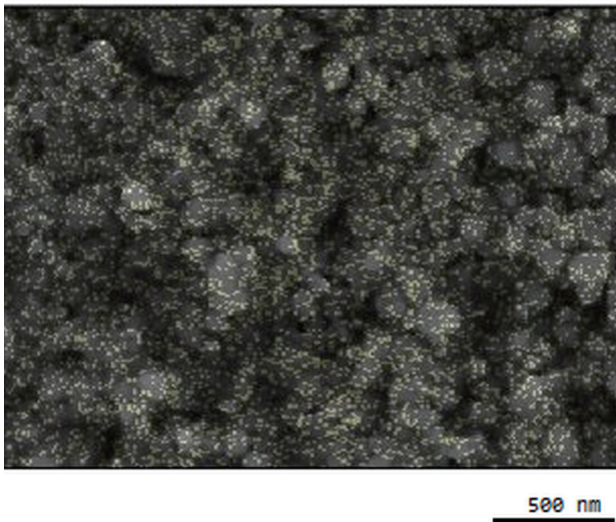


**Fig. 6.** EDX image of the fluorine-labeled KAB specimen. The pale yellow dots represent fluorine atoms.

### 3. Results

#### 3.1. Three-point bending test

The elastic modulus of the KAB was 8.2 GPa for the before-immersion group and 6.9 GPa for the after-immersion group. The elastic modulus of the EMB was 3 GPa for the before-immersion group and 2.7 GPa for the after-immersion group.

#### 3.2. XPS investigation

An EDX image of the KAB is shown in **Figure 6**. The pale yellow dots represent fluorine atom locations. Because the fluorine atoms settled near the fillers where the silane coupling agent was covered, the labeling process was considered to be successful.

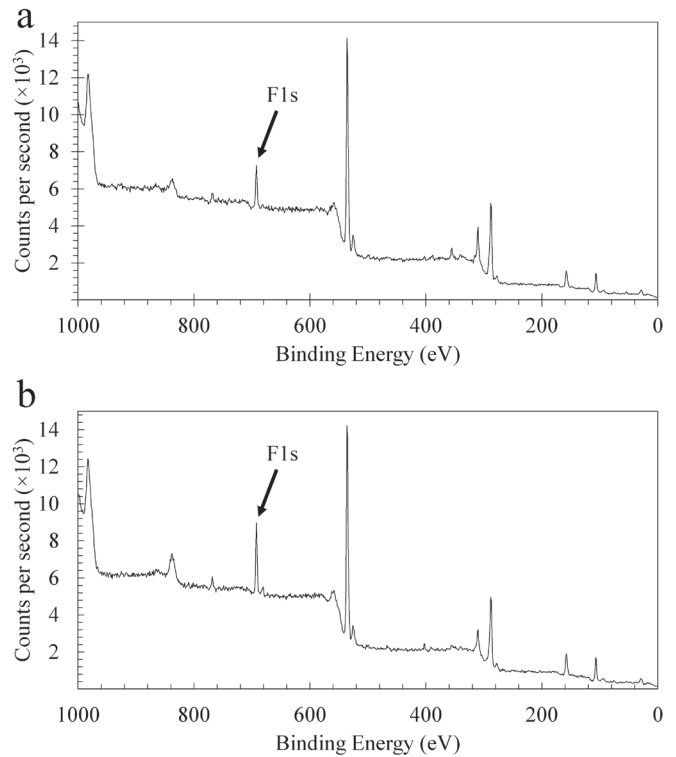


**Fig. 7.** XPS spectra of the fluorine-labeled KAB (a) before and (b) after immersion in water

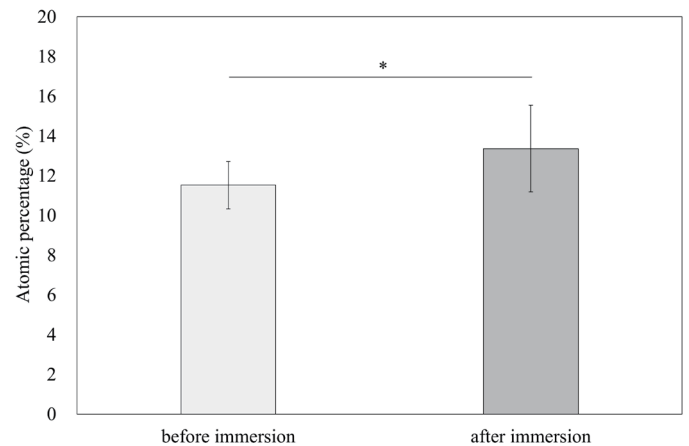


**Fig. 8.** Atomic percentages of F1s in the fluorine-labeled KAB before and after immersion (Student's *t*-test,  $n = 5$ ,  $*p < 0.05$ )

The XPS F1s peak at 692 eV, representing PFODMCS attached to the hydroxyl group, is shown in **Figure 7**. The atomic percentage of F1s for the after-immersion group was 14.31%, which was significantly greater than that for the before-immersion group (11.52%) (**Fig. 8**), suggesting that hydrolysis of the silane coupling layer occurred during water immersion.

#### 3.3. In silico analysis

The coupling ratios and corresponding elastic moduli of the silane coupling layers are summarized in **Table 2**. The unknown cou-

**Table 2.** Coupling ratios and corresponding elastic moduli of the silane coupling layer

Coupling ratio (%)	100	95	90	85	80	75	70	65	60	55	50
Elastic modulus (GPa)	2.00	1.74	1.53	1.37	1.22	1.10	1.00	0.88	0.78	0.69	0.60

**Table 3.** Prediction of the coupling ratio.  $EM_{\text{matrix}}$ ,  $EM_{\text{silane}}$ ,  $EM_{\text{model}}$  and coupling ratio were experimental data of this study.  $EM_{\text{filler}}$  is referred previous study[28].

	$EM_{\text{matrix}}$ (GPa)	$EM_{\text{filler}}$ (GPa)	$EM_{\text{silane}}$ (GPa)	$EM_{\text{model}}$ (GPa)	Coupling ratio (%)
Before immersion	3	72	$1.16 \pm 0.05$	$8.19 \pm 0.11$	$78.2 \pm 1.64$
After immersion	2.7	72	$0.92 \pm 0.04$	$6.89 \pm 0.15$	$68.4 \pm 0.89$

(n = 5)

pling ratio for a particular elastic modulus was interpolated using the relation between the coupling ratio and elastic modulus. By repeated calculation, the elastic modulus of the silane coupling layer was determined to be  $1.16 \pm 0.05$  GPa for the before-immersion group. For this elastic modulus, the coupling ratio was predicted to be  $78.2 \pm 1.64\%$ . For the after-immersion group, the elastic modulus of the silane coupling layer was determined to be  $0.92 \pm 0.04$  GPa, corresponding to  $68.4\% \pm 0.89\%$  coupling ratio (Table 3).

#### 4. Discussion

This study was performed to clarify how water absorption of CAD/CAM resin composites quantitatively affects the silane coupling ratio. Because CAD/CAM resin composites are typically used in humid conditions, clarifying the change of the physical properties under these conditions is important.

The elastic moduli of both the KAB and EMB decreased with water absorption. Because the EMB was manufactured under the same conditions as the matrix resin area of the KAB, one of factors for the performance deterioration of the CAD/CAM resin composite by water absorption was degradation of the matrix resin. In the matrix resin, water absorption is described by dual-mode theory, which considers that water molecules absorb in two ways[31]. The first is ordinary molecular dissolution in the matrix resin and the second is physical entrapment in polymer micro-voids. The absorbed water is molecularly dispersed in the matrix resin and acts as a plasticizer, causing swelling of the polymer. The amount of this absorbed water depends on the equilibrium volume, physicochemical affinity to the polymer, and resistance of the polymer chains to swelling deformation stress. This water serves as a proton donor and causes chemical reaction with the matrix resin or silane coupling agent. Alternatively, the water molecules that are accommodated in the micro-voids form hydrogen bonds, acting as filler particles. These water molecules increase the elastic modulus of the bulk block after water absorption[32,33]. In this study, the water molecules functioned as a proton donor rather than as a filler, reducing the elastic modulus. Degradation of the silane coupling layer is also considered to be an important factor for deterioration of CAD/CAM resin composites. Water molecules likely enter the silane-treated layers and gradually hydrolyze the siloxane bonds between the fillers and water molecules, hydrating the resultant hydroxysilyl group[19,34,35].

XPS investigation with a fluorine-labeling technique was performed to evaluate the amount of hydroxyl groups[36–38]. The peroxodisulfate can be activated by energy to form sulfate radical and effective degradation of contaminants [39]. An appropriate activating method of the peroxodisulfate was recruited from the previ-

ous study [37]. In this study, the 99% ethanol was used for PFODMCS solvent. The chlorosilanes including PFODMCS reacts with the alcohol producing an alkoxy silanes and HCl. Part of the HCl reacts with the alcohol to produce alkyl halide and water. The water causes formation of silanol from alkoxy silanes. The hydroxyl groups in silanol make hydrogen bond with hydroxyl group of the substrate. Then during 2 hours of drying and curing process, covalent linkages are formed with the substrate with concomitant loss of water. The binding energy of the electron in the 1s orbital of fluorine (F1s) was used to confirm changes in the hydroxyl group. The F1s peak in the XPS spectrum and the greater atomic percentage in the after-immersion group than the before-immersion group suggest that hydrolysis in the silane coupling layer occurred during water immersion. Although it has been reported that XPS analysis can be used to qualitatively assess the target atom[40–42], in the case of CAD/CAM resin composites, hydroxyl groups develop on the silane coupling layer as well as on the surface of the fillers. Therefore, assessing the absolute amount of the hydrolyzed silane coupling layer is impractical. However, considering the fact that silica fillers are chemically stable in water, it can be assumed that the amount of hydroxyl groups on the silica filler is constant. The XPS analysis results can be considered to be valid even if the absolute amount of hydrolysis cannot be estimated.

In a previous study, it was reported that a decrease in the elastic modulus occurred in conjunction with a decrease in the silane coupling ratio[43]. When this result is combined with the XPS results, it can be deduced that water immersion may cause reduction of the elastic modulus of the bulk block by impairment of the silane coupling layer, as well as the matrix resin

The elastic modulus of the 75.5% silane coupling model decreased to 16.8% compared with that of the 100% silane coupling model. This result supports that excessive water uptake may further decrease the elastic modulus of resin composites[8] because of hydrolytic degradation[44]. The decrease in the elastic modulus may induce debonding of CAD/CAM resin composite prosthetics by deformation of the margin[45].

After 7 days of immersion of the KAB in water, the silane coupling ratio decreased to 68.4%, suggesting that 9.8% of the silane coupling layer was hydrolyzed. The alkoxy group of silane changed to a silanol group by activation, which generates a covalent bond or a hydrogen bond on the surface of inorganic fillers[19]. The covalent bonds between the alkoxy group and inorganic filler stabilize the organic/inorganic interface[46]. However, interfacial hydrogen bonds are broken in a humid environment[47]. Furthermore, the organofunctional groups of silane that form an ester bond with the matrix resin are hydrolyzable[46].

The reduction of the chemico-mechanical value for each component showed a similar tendency to the bulk block. However, after 7 days, the overall mechanical properties non-linearly decreased [29]. Therefore, the long-term change of the silane coupling ratio should be further investigated.

## 5. Conclusions

In this study, water absorption in CAD/CAM resin composites resulted in reduction of the elastic modulus and hydrolysis of the silane coupling layer. Hydrolysis of the silane coupling layer during water immersion was verified to be one of the reasons for reduction of the elastic modulus of CAD/CAM resin composites. The *in vitro* and *in silico* approaches established in this study were able to predict the silane coupling ratio of CAD/CAM resin composites, and they clearly showed that the silane coupling ratio decreased by water absorption.

## Acknowledgments

This research was supported by a Grant-in-Aid for Scientific Research (No. JP19K10244) from the Japan Society for the Promotion of Science (JSPS). The authors thank Kuraray Noritake Dental for providing materials. We thank Tim Cooper, PhD, from Edanz (<https://jp.edanz.com/ac>) for editing a draft of this manuscript.

## Conflicts of Interest

The authors declare that they have no conflict of interest.

## References

- Miyazaki T, Hotta Y, Kunii J, Kuriyama S, Tamaki Y. A review of dental CAD/CAM: current status and future perspectives from 20 years of experience. *Dent Mater J*. 2009;28:44–56. <https://doi.org/10.4012/dmj.28.44>, PMID:19280967
- Davidowitz G, Kotick PG. The use of CAD/CAM in dentistry. *Dent Clin North Am*. 2011;55:559–70, ix. <https://doi.org/10.1016/j.cden.2011.02.011>, PMID:21726690
- van Noort R. The future of dental devices is digital. *Dent Mater*. 2012;28:3–12. <https://doi.org/10.1016/j.dental.2011.10.014>, PMID:22119539
- Duret F, Blouin JL, Duret B. CAD-CAM in dentistry. *J Am Dent Assoc*. 1988;117:715–20. <https://doi.org/10.14219/jada.archive.1988.0096>, PMID:3058771
- Duret F, Preston JD. CAD/CAM imaging in dentistry. *Curr Opin Dent*. 1991;1:150–4. PMID:1777659
- Ferracane JL. Resin composite—state of the art. *Dent Mater*. 2011;27:29–38. <https://doi.org/10.1016/j.dental.2010.10.020>, PMID:21093034
- Pratap B, Gupta RK, Bhardwaj B, Nag M. Resin based restorative dental materials: characteristics and future perspectives. *Jpn Dent Sci Rev*. 2019;55:126–38. <https://doi.org/10.1016/j.jdsr.2019.09.004>, PMID:31687052
- Ruse ND, Sadoun MJ. Resin-composite blocks for dental CAD/CAM applications. *J Dent Res*. 2014;93:1232–4. <https://doi.org/10.1177/0022034514553976>, PMID:25344335
- Piconi C, Maccauro G. Zirconia as a ceramic biomaterial. *Biomaterials*. 1999;20:1–25. [https://doi.org/10.1016/S0142-9612\(98\)00010-6](https://doi.org/10.1016/S0142-9612(98)00010-6), PMID:9916767
- Goumans TPM, Wander A, Brown WA, Catlow CRA. Structure and stability of the (001)  $\alpha$ -quartz surface. *Phys Chem Chem Phys*. 2007;9:2146–52. <https://doi.org/10.1039/B701176H>, PMID:17464397
- Wolanov Y, Shurki A, Prikhodchenko PV, Tripol'skaya TA, Novotortsev VM, Pedahzur R, et al. Aqueous stability of alumina and silica perhydrate hydrogels: experiments and computations. *Dalton Trans*. 2014;43:16614–25. <https://doi.org/10.1039/C4DT01024H>, PMID:24965747
- Endo T, Finger WJ, Kanehira M, Utterodt A, Komatsu M. Surface texture and roughness of polished nanofill and nanohybrid resin composites. *Dent Mater J*. 2010;29:213–23. <https://doi.org/10.4012/dmj.2009-019>, PMID:20379033
- Mitra SB, Wu D, Holmes BN. An application of nanotechnology in advanced dental materials. *J Am Dent Assoc*. 2003;134:1382–90. <https://doi.org/10.14219/jada.archive.2003.0054>, PMID:14620019
- Satterthwaite JD, Vogel K, Watts DC. Effect of resin-composite filler particle size and shape on shrinkage-strain. *Dent Mater*. 2009;25:1612–5. <https://doi.org/10.1016/j.dental.2009.08.012>, PMID:19801168
- Lu H, Lee YK, Oguri M, Powers JM. Properties of a dental resin composite with a spherical inorganic filler. *Oper Dent*. 2006;31:734–40. <https://doi.org/10.2341/05-154>, PMID:17153985
- Okada K, Kameya T, Ishino H, Hayakawa T. A novel technique for preparing dental CAD/CAM composite resin blocks using the filler press and monomer infiltration method. *Dent Mater J*. 2014;33:203–9. <https://doi.org/10.4012/dmj.2013-329>, PMID:24583649
- Söderholm KJM, Shang SW. Molecular orientation of silane at the surface of colloidal silica. *J Dent Res*. 1993;72:1050–4. <https://doi.org/10.1177/00220345930720061001>, PMID:8388415
- Chen JH, Matsumura H, Atsuta M. Effect of etchant, etching period, and silane priming on bond strength to porcelain of composite resin. *Oper Dent*. 1998;23:250–7. PMID:9863446
- Nihei T. Dental applications for silane coupling agents. *J Oral Sci*. 2016;58:151–5. <https://doi.org/10.2334/josnusd.16-0035>, PMID:27349534
- Hooshmand T, Keshvad A, van Noort R. XPS Analysis of Silane Films on the Surface of a Dental Ceramic. *J Adhes Sci Technol*. 2009;23:1085–95. <https://doi.org/10.1163/156856109X432695>
- Pantano CG, Wittberg TN. XPS analysis of silane coupling agents and silane-treated E-glass fibers. *Surf Interface Anal*. 1990;15:498–501. <https://doi.org/10.1002/sia.740150809>
- Söderholm KJ, Zigan M, Ragan M, Fischlschweiger W, Bergman M. Hydrolytic degradation of dental composites. *J Dent Res*. 1984;63:1248–54. <https://doi.org/10.1177/00220345840630101701>, PMID:6592209
- Sideridou I, Tserki V, Papanastasiou G. Study of water sorption, solubility and modulus of elasticity of light-cured dimethacrylate-based dental resins. *Biomaterials*. 2003;24:655–65. [https://doi.org/10.1016/S0142-9612\(02\)00380-0](https://doi.org/10.1016/S0142-9612(02)00380-0), PMID:12437960
- Øysaet D, Ruyter IE. Composites for use in posterior teeth: mechanical properties tested under dry and wet conditions. *J Biomed Mater Res*. 1986;20:261–71. <https://doi.org/10.1002/jbm.820200214>, PMID:3957963
- Söderholm KJM, Roberts MJ. Influence of water exposure on the tensile strength of composites. *J Dent Res*. 1990;69:1812–6. <https://doi.org/10.1177/00220345900690120501>, PMID:2250085
- Francfort GA. Homogenization and Linear Thermoelasticity. *SIAM J Math Anal*. 1983;14:696–708. <https://doi.org/10.1137/0514053>
- Guedes J, Kikuchi N. Preprocessing and postprocessing for materials based on the homogenization method with adaptive finite element methods. *Comput Methods Appl Mech Eng*. 1990;83:143–98. [https://doi.org/10.1016/0045-7825\(90\)90148-F](https://doi.org/10.1016/0045-7825(90)90148-F)
- Yamaguchi S, Inoue S, Sakai T, Abe T, Kitagawa H, Imazato S. Multi-scale analysis of the effect of nano-filler particle diameter on the physical properties of CAD/CAM composite resin blocks. *Comput Methods Biomech Biomed Engin*. 2017;20:714–9. <https://doi.org/10.1080/10255842.2017.1293664>, PMID:28387166
- Lee C, Yamaguchi S, Ohta K, Imazato S. Mechanical properties of computer-aided design/computer-aided manufacturing resin composites assuming perfect silane coupling using *in silico* homogenization of cryo-electron microscopy images. *J Prosthodont Res*. 2019;63:90–4. <https://doi.org/10.1016/j.jpor.2018.09.001>, PMID:30529229
- Wang BG, Yamaguchi T, Nakao SI. Solvent diffusion in amorphous glassy polymers. *J Polym Sci, B, Polym Phys*. 2000;38:846–56. [https://doi.org/10.1002/\(SICI\)1099-0488\(20000315\)38:6<846::AID-POLB5>3.0.CO;2-B](https://doi.org/10.1002/(SICI)1099-0488(20000315)38:6<846::AID-POLB5>3.0.CO;2-B)
- Patil RD, Mark JE, Apostolov A, Vassileva E, Fakirov S. Crystallization of water in some crosslinked gelatins. *Eur Polym J*. 2000;36:1055–61. [https://doi.org/10.1016/S0014-3057\(99\)00144-5](https://doi.org/10.1016/S0014-3057(99)00144-5)
- Ping ZH, Nguyen QT, Chen SM, Zhou JQ, Ding YD. States of water in different hydrophilic polymers— DSC and FTIR studies. *Polymer (Guildf)*. 2001;42:8461–7. [https://doi.org/10.1016/S0032-3861\(01\)00358-5](https://doi.org/10.1016/S0032-3861(01)00358-5)
- Debnath S, Wunder SL, McCool JI, Baran GR. Silane treatment effects on glass/resin interfacial shear strengths. *Dent Mater*. 2003;19:441–8. [https://doi.org/10.1016/S0109-5641\(02\)00089-1](https://doi.org/10.1016/S0109-5641(02)00089-1), PMID:12742441

- [34] Brochier Salon M-C, Bayle PA, Abdelmouleh M, Boufi S, Belgacem MN. Kinetics of hydrolysis and self condensation reactions of silanes by NMR spectroscopy. *Colloids Surf A Physicochem Eng Asp.* 2008;312:83–91. <https://doi.org/10.1016/j.colsurfa.2007.06.028>
- [35] Dang TA, Gnanasekaran R, Deppe DD. Quantification of surface hydroxides using chemical labeling and XPS. *Surf Interface Anal.* 1992;18:141–6. <https://doi.org/10.1002/sia.740180214>
- [36] McCafferty E, Wightman JP. Determination of the concentration of surface hydroxyl groups on metal oxide films by a quantitative XPS method. *Surf Interface Anal.* 1998;26:549–64. [https://doi.org/10.1002/\(SICI\)1096-9918\(199807\)26:8<549::AID-SIA396>3.0.CO;2-Q](https://doi.org/10.1002/(SICI)1096-9918(199807)26:8<549::AID-SIA396>3.0.CO;2-Q)
- [37] Yoshida Y, Shirai K, Nakayama Y, Itoh M, Okazaki M, Shintani H, et al. Improved filler-matrix coupling in resin composites. *J Dent Res.* 2002;81:270–3. <https://doi.org/10.1177/154405910208100409>, PMID:12097312
- [38] Dupraz AMP, de Wijn JR, v d Meer SA, de Groot K. Characterization of silane-treated hydroxyapatite powders for use as filler in biodegradable composites. *J Biomed Mater Res.* 1996;30:231–8. [https://doi.org/10.1002/\(SICI\)1097-4636\(199602\)30:2<231::AID-JBM13>3.0.CO;2-P](https://doi.org/10.1002/(SICI)1097-4636(199602)30:2<231::AID-JBM13>3.0.CO;2-P), PMID:9019488
- [39] Zhang BT, Zhang Y, Teng Y, Fan M. Sulfate Radical and Its Application in Decontamination Technologies. *Crit Rev Environ Sci Technol.* 2015;45:1756–800. <https://doi.org/10.1080/10643389.2014.970681>
- [40] Dietrich PM, Streeck C, Glamsch S, Ehlert C, Lippitz A, Nutsch A, et al. Quantification of silane molecules on oxidized silicon: are there options for a traceable and absolute determination? *Anal Chem.* 2015;87:10117–24. <https://doi.org/10.1021/acs.analchem.5b02846>, PMID:26334589
- [41] Lee C, Kashima K, Ichikawa A, Yamaguchi S, Imazato S. Influence of hydrolysis degradation of silane coupling agents on mechanical performance of CAD/CAM resin composites: *In silico* multi-scale analysis. *Dent Mater J.* 2020;39:803–7. <https://doi.org/10.4012/dmj.2019-223>, PMID:32404566
- [42] Ferracane JL. Hygroscopic and hydrolytic effects in dental polymer networks. *Dent Mater.* 2006;22:211–22. <https://doi.org/10.1016/j.dental.2005.05.005>, PMID:16087225
- [43] Rosentritt M, Preis V, Behr M, Hahnel S. Influence of preparation, fitting, and cementation on the vitro performance and fracture resistance of CAD/CAM crowns. *J Dent.* 2017;65:70–5. <https://doi.org/10.1016/j.jdent.2017.07.006>, PMID:28734997
- [44] Witucki GL. A Silane Primer - Chemistry and Applications of Alkoxy Silanes. *J Coatings Technology.* 1993;65:57–60.
- [45] Choi S, Maul S, Stewart A, Hamilton HR, Douglas EP. Effect of silane coupling agent on the durability of epoxy adhesion for structural strengthening applications. *Polym Eng Sci.* 2013;53:283–94. <https://doi.org/10.1002/pen.23261>
- [46] Koin PJ, Kilislioglu A, Zhou M, Drummond JL, Hanley L. Analysis of the degradation of a model dental composite. *J Dent Res.* 2008;87:661–5. <https://doi.org/10.1177/154405910808700712>, PMID:18573987
- [47] Arikawa H, Kuwahata H, Seki H, Kanie T, Fujii K, Inoue K. Deterioration of mechanical properties of composite resins. *Dent Mater J.* 1995;14:78–83,104. <https://doi.org/10.4012/dmj.14.78>, PMID:8940548



This is an open-access article distributed under the terms of Creative Commons Attribution-NonCommercial License 4.0 (CC BY-NC 4.0), which allows users to distribute and copy the material in any format as long as credit is given to the Japan Prosthodontic Society. It should be noted however, that the material cannot be used for commercial purposes.